Mechanism for translocation of fluoroquinolones across lipid membranes

Oana Cramariuc [a,*], Tomasz Rog [a], Matti Javanainen [a], Luca Monticelli [b,c],
Anna V. Polishchuk [d], Ilpo Vattulainen [a,e]

[a] Department of Physics, Tampere University of Technology, P.O. Box 692, FI-33101 Tampere, Finland
[b] INSERM URM-S665, DSIMB 75015, Paris, France
[c] Université Paris Diderot-Paris 7, UFR Life Sciences, Paris, France
[d] Institute of Chemistry, Far-Eastern Branch of the Russian Academy of Sciences, pr.100-let Vladivostoku, 159, Vladivostok, 690022, Russia
[e] MEMPHYS-Centre for Biomembrane Physics, University of Southern Denmark, Odense, Denmark

ARTICLE INFO

ABSTRACT

Classical atom-scale molecular dynamics simulations, constrained free energy calculations, and quantum mechanical (QM) calculations are employed to study the diffusive translocation of ciprofloxacin (CPFX) across lipid membranes. CPFX is considered here as a representative of the fluoroquinolone antibiotics class. Neutral and zwitterionic CPFX coexist at physiological pH, with the latter being predominant. Simulations reveal that only the neutral form permeates the bilayer, and it does so through a novel mechanism that involves dissolution of concerted stacks of zwitterionic ciprofloxacins. Subsequent QM analysis of the observed molecular stacking shows the important role of partial charge neutralization in the stacks, highlighting how the zwitterionic form of the drug is neutralized for translocation. The findings propose a translocation mechanism in which zwitterionic CPFX molecules approach the membrane in stacks, but they diffuse through the membrane as neutral CPFX monomers due to intermolecular transfer of protons favored by partial solvation loss. The mechanism is expected to be of importance in the permeation and translocation of a variety of ampholitic drugs with stacking tendencies.

© 2012 Elsevier B.V. All rights reserved.

1. Introduction

Fluoroquinolones (FQs) developed by modifications of an old antibacterial agent (nalidixic acid) have since the mid-1980s dramatically changed the antibiotic market. Their discovery has generated considerable clinical and scientific interest due to their broad antibacterial spectrum with less resistance, rapid bactericidal effect, and good oral absorption properties. As such, ciprofloxacin (CPFX, see Fig. 1), which belongs to the second generation of FQs, is one of the most widely used antibiotics for the treatment of respiratory, urinary, and enteric infections. Very importantly, similarly to other clinically antibacterial drugs, FQs have intracellular target sites. Therefore as a first hypothesis their broad spectrum of action is due to their ability to cross bacterial envelopes and cytoplasmic membranes [1], and consequently the antibacterial activity of FQs appears to result from the combination of efficient cellular membrane penetration and DNA gyrase inhibiting activity. The central

issue at the moment is that the molecular-scale entry mechanism of these drugs through membranes is still under debate, see below.

Membrane proteins play an important role in the uptake of FQs by Gram-negative bacteria through their outer membrane [2,3]. Meanwhile, translocation through the inner membrane takes place via passive diffusion, both in Gram-negative bacteria and in the membrane of Gram-positive organisms [1,4]. Recent parallel artificial membrane permeability assay studies have also proven that as much as 80% of CPFX passively permeates through the membrane, while paracellular permeability through pores is responsible for the rest 20% [5]. Considering the passive diffusion of FQs, one has to take into account that they have two ionization states coexisting at physiological pH: a *zwitterionic* (and overall uncharged) form with a significant dipole, and an uncharged *neutral* form (with negligible/minor dipole; see Fig. 1) [6–9]. Despite their predominant zwitterionic character [7–9] FQs are known to cross membranes via passive transport. This view is also supported by various membrane vesicle and liposome experiments [10–12], which suggest that the zwitterionic species is responsible for the diffusion through the cellular membrane [10].

It is common knowledge that the intrinsic lipophilicity of neutral species is greater than that of cations and anions. In contrast, much controversy surrounds the lipophilicity of zwitterions, which is very low according to some authors but marked according to others [6], and no direct experimental method is available to determine separately their individual partition coefficients. What is more, inter-
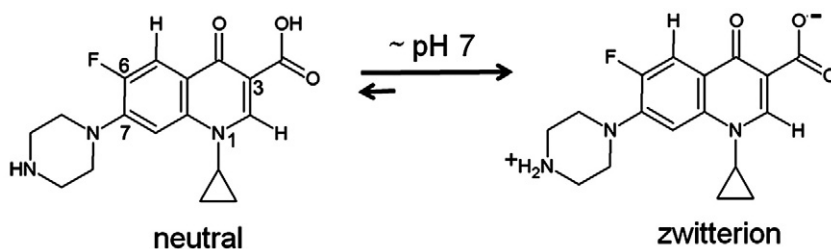
Fig. 1. Molecular structures of neutral and zwitterionic CPFX. The central structural unit of CPFX is a quinolone ring with the fluorine atom at C-6, a piperazine moiety at C-7, a cyclopropyl ring at position 1 and a carboxyl group at position 3.

and intramolecular effects like charge delocalization, internal electrostatic bonds, and folding often increase lipophilicity [6,13], and these effects could make a difference also for the zwitterionic form of CPFX.

Taken together, the available data suggest that not only the small fraction of neutral-form FQs translocates through the lipid bilayer. Instead, in some unknown manner diffusion of zwitterionic FQs across a bilayer does take place, too, to account for the high portion of the translocated drug. Importantly, to understand the action of FQs in general, one first has to unravel its translocation mechanism.

To this end, we use here atomistic molecular dynamics (MD) simulations to study the behavior of both neutral and zwitterionic CPFX in water as well as their translocation across a lipid bilayer composed of unsaturated phosphatidylcholine (PC) molecules. While many bacterial membranes consist of a mixture of phosphatidylethanolamine (PE) and phosphatidylglycerol (PG) lipids, the PC bilayer considered here offers a good starting point for our simulations, as it is the most studied and best understood membrane model overall. Furthermore, we determine the free energy profile of CPFX across the lipid bilayer and use it to discuss permeation characteristics of the drug. Finally, these classical simulations are complemented with quantum mechanical (QM) calculations at density functional theory (DFT) level to address questions raised by atomistic MD simulations and to propose a complete picture of the penetration process.

2. Computational methods and models

2.1. Molecular dynamics simulations

Atomic-scale MD simulations of neutral and zwitterionic CPFX molecules were performed both in the presence and in the absence of 1,2-Dilinoleoyl-sn-Glycero-3-phosphatidylcholine lipid bilayer. We used a previously equilibrated lipid bilayer [14] consisting of 128 PC molecules, which are phospholipids with di-unsaturated hydrocarbon chains, each including 18 carbons with double bonds at positions 9 and 12 (linoleic acid, 18:2c9,12). Long tails were chosen as they ensure that the bilayer is in the fluid phase. Fully hydrated bilayers with either ~3250 or ~7500 water molecules were considered, resulting in two different thicknesses for the water layer. In the starting configuration 10 CPFX molecules were distributed randomly in the water phase.

We used the all-atom OPLS (optimized parameters for liquid simulations) force field [15–18] with partial charges on the PC head group taken from Takaoka et al. [19]. Details of the force field implementation are given in ref. [14]. It was shown by Rog et al. that this parameterization reproduces correctly the properties of lipid bilayers composed of the given phosphatidylcholines [20]. Partial atomic charges for CPFX were derived in line with the OPLS methodology by fitting them to the electrostatic potential using the RESP procedure [21]. First, the Merz–Kollman molecular electrostatic potential (MEP) was computed for the optimized molecule structure [22]. The MEP calculations were performed at Hartree–Fock level by employing the 6–31G* basis set using the Gaussian 03 program [23]. The charge fitting was done automatically using the RESP ESP charge derived (R.E.D.) software version

III (a, b, c). Water was described by the TIP3P model, which is compatible with the OPLS parameterization [24].

Simulations in every system were performed using the GROMACS software package [25,26] over a time scale of 300 ns. The steepest-descent algorithm was employed to minimize the energies of the initial structures prior to actual MD simulations. Periodic boundary conditions were used in all directions with the minimum image convention. The LINCS algorithm [27] was employed to constrain covalent bonds, and the time step was set to 2 fs. The simulations were carried out at constant pressure (1 bar) using semi-isotropic control [28] with a time constant of 2 ps. The bilayer systems were kept in the fluid phase at 310 K with the weak coupling Berendsen scheme [28] using a time constant of 0.2 ps. The Lennard–Jones interactions were cut off at 1.0 nm, and for the electrostatic interactions we employed the particle mesh Ewald method with a real space cutoff of 1.0 nm. The list of non-bonded pairs was updated every 10th time step. The simulation protocol used in this study has been successfully applied in many previous MD simulation studies of lipid bilayers [14,20,29–31].

2.2. Free energy profiles from z-constraint calculations

In order to obtain detailed information on the energetics of CPFX partitioning, a set of simulations with constraints was performed for both the zwitterionic and the neutral forms of CPFX. The center of mass of CPFX was constrained in z direction (along the membrane normal direction) at a total of 35 different locations from the membrane core to the bulk water phase with a spacing of 0.1 nm. The starting configurations for these windows were obtained by first pulling the CPFX molecule from the water phase to the membrane center with an umbrella potential, whose reference point was moved at a constant velocity. The frames with correct distances between the membrane center of mass and the CPFX molecule were then extracted from the obtained trajectory.

Each window was simulated for 15 ns, and the latter half was used in the analysis. A rather long equilibration time was employed to ensure that the molecule probed its equilibrium orientations within the membrane. Even though the z coordinate of the CPFX molecule was constrained in the simulations, the molecule was allowed to diffuse freely in the xy-plane. The value of the force experienced by CPFX in z direction was saved every 10 steps. The excess free energy with respect to water at a chosen depth z from the bulk water phase was obtained through integration of the mean of this force in the direction of pulling. All free energy profiles were calculated for one lipid leaflet and have been symmetrized. Other simulation parameters were kept at the same values as in the equilibrium MD simulations described in Section 2.2.

2.3. Quantum mechanical calculations

Density functional calculations (DFT) with the gradient corrected BLYP (Becke–Lee–Yang–Parr) functional and the double zeta valence with polarization (DZVP) basis set, as implemented in the Turbomole software package [32], were employed in all calculations. The Grimme's

correction scheme was used to compensate for the missing long-range interactions [33,34]. The conductor-like screening model (COSMO) model with a dielectric constant of 80 was employed to account for the water phase [35,36]. Smaller dielectric constants ($\varepsilon_r = 2, 5, 10, 15, 20, 30, 40, 50$) were used to test the stability of the stacked zwitterionic CPFX in different environments. Random stacks of head-to-tail orientations were selected from (classical) MD simulations and their structure was optimized at the DFT level. The optimized structure was roughly the same, regardless of small differences in the initial relative orientation. The electrostatic potential was calculated by employing the same functional as for geometry optimizations with the TZVP basis set but within the Gaussian 09 computational package [23].

3. Results and discussion

3.1. Atomistic simulations of neutral ciprofloxacin

We first examined the interaction of neutral CPFX with the PC bilayer. The distribution of CPFX molecules along the axis perpendicular to the bilayer showed that insertion into the head group region takes place within a few tens of nanoseconds (Fig. 2a).

In the beginning, some molecules entered symmetrically the two sides of the bilayer as shown by the relatively symmetric distribution obtained in the beginning of the simulation (Fig. 2a). However, at long times a clear accumulation of the remaining CPFX on one side of the bilayer was observed, as is highlighted by a more asymmetric distribution (Fig. 2b). The molecules in the bilayer positioned themselves in the head group region at approximately 1.5 nm from the membrane center, right under the lipid head groups. Another local maximum in the CPFX distribution is observed in the water phase right above the water–membrane interface at about 3 nm from the membrane center. The free energy barrier between these two local peaks is small given the fact that CPFX molecules readily diffused through the head group region within the given simulation time. However, the situation is very different in the membrane hydrophobic region. Considering that the density of CPFX in the membrane center is marginal, there is reason to assume that there is a considerable free energy barrier in the middle of the membrane. We will come back to this topic below (see Fig. 5).

Snapshots in Fig. 3, taken after ~200 ns of MD simulation, agree with our interpretation of the density distribution data, showing several CPFX molecules in the polar head group region, close to the hydrophobic chains of PCs. Most interestingly, there is a stacked aggregate of CPFX approaching the bilayer (Fig. 3a), which explains the accumulation seen in the density distribution in Fig. 2b. Hydrogen bonds with the lipid head groups appeared to facilitate the adsorption of the CPFX stack onto the water–bilayer interfaces. The hydrogen bonds occurred

in the beginning of the adsorption process mainly between the nitrogen atoms of the 7-piperazine side chain and the oxygen atoms in the phosphate moiety of the lipid head group. At longer times, as the stack of CPFX molecules started to enter the membrane (Fig. 3b), a significant number of hydrogen bonds were formed between the carboxylic group of CPFX and the ester groups of PC. None of the other heteroatoms of CPFX, such as, e.g., fluorine or carbonyl oxygen, appeared to participate in the hydrogen bond formation. The pattern of these hydrogen bonds points to the role of piperazine in initiating the translocation process. Indeed, the development of pipemidic acid with the addition of a 7-piperazine side chain in the late 1960s allowed better penetration of the bacterial cell wall, conferring improved activity against *Pseudomonas aeruginosa* as well as some Gram-positive bacteria [37–40]. Nowadays, the majority of the FQ family members contain piperazine or substituted piperazine, which has been shown to enhance both permeability and potency.

Moving on, as the stack of neutral CPFX molecules moved deeper, crossing the ester bond region of a lipid bilayer, the stack ruptured (Fig. 3c). During the final stage of the simulation, neutral CPFX molecules were observed to remain in the membrane hydrophobic region as monomers. It is noteworthy that we did not identify actual translocation events where a neutral CPFX molecule would have crossed the membrane center by moving from one leaflet to the other. Considering the density distributions in Fig. 2, this is not surprising, since the density of CPFX in the membrane center was observed to be marginal.

Let us finally come back to the stack formation process. Clearly, neutral ciprofloxacin molecules in the water phase exhibited a pronounced tendency to associate in stacks. It is in fact in the form of columnar stacks that the molecules interacted in the MD simulations with the lipid bilayer and started to enter the head group region as demonstrated by Fig. 3. Experimentally stacking of CPFX has been observed in the interior of liposomes, where the molecules have been found to self-associate without precipitating even at concentrations that exceed the solubility in aqueous solutions [11]. Stacking appears to be an intrinsic property of FQs occurring due to π–π interactions and hydrogen bonding, as revealed by X-ray diffraction studies [41] and spectroscopic measurements [42]. Further, our MD simulations performed with only CPFX in water revealed that stack formation is both a dynamic and a concentration dependent process. The CPFX molecules associated in stacks which both formed and broke apart over the entire length of the simulation, and whose size increased when the concentration was changed from 0.04 M to 0.08 M.

3.2. Atomistic simulations of zwitterionic ciprofloxacin

Next, we considered the zwitterionic form of CPFX. Fig. 4a presents a snapshot taken from the end of the simulation, showing aggregates of two or more zwitterions in the water phase. While neutral CPFX entered and stayed in the lipid bilayer, zwitterionic CPFX only formed aggregates, which remained in the water phase. Very few molecules approached the lipid head groups during the 300 ns simulation time as evidenced by the density distribution in Fig. 4b. Presumably the large charges on carboxyl and piperazine, the substituents shown to be mainly involved in the interaction of the drug with the lipid bilayer, prevent zwitterions from entering the bilayer.

Fig. 4b clearly shows that the number density of zwitterionic CPFX in the membrane hydrophobic region is vanishingly small, and is considerably smaller compared to the neutral case. The free energy barrier associated with translocation of zwitterionic CPFX monomers is therefore expected to be substantially larger compared to the barrier for neutral CPFX monomers.

As in the case of neutral CPFX, also for zwitterionic molecules stacking takes place independently of the bilayer and depends on the CPFX concentration. At concentrations of 0.04 M we observed formation of only small two-molecule stacks. At higher concentration
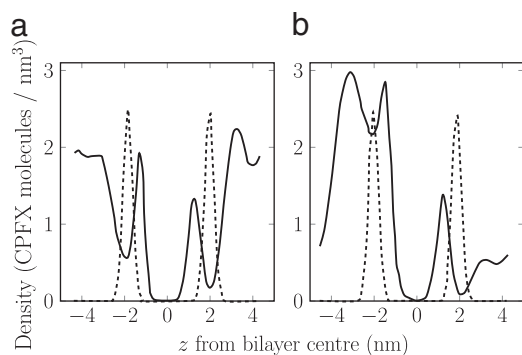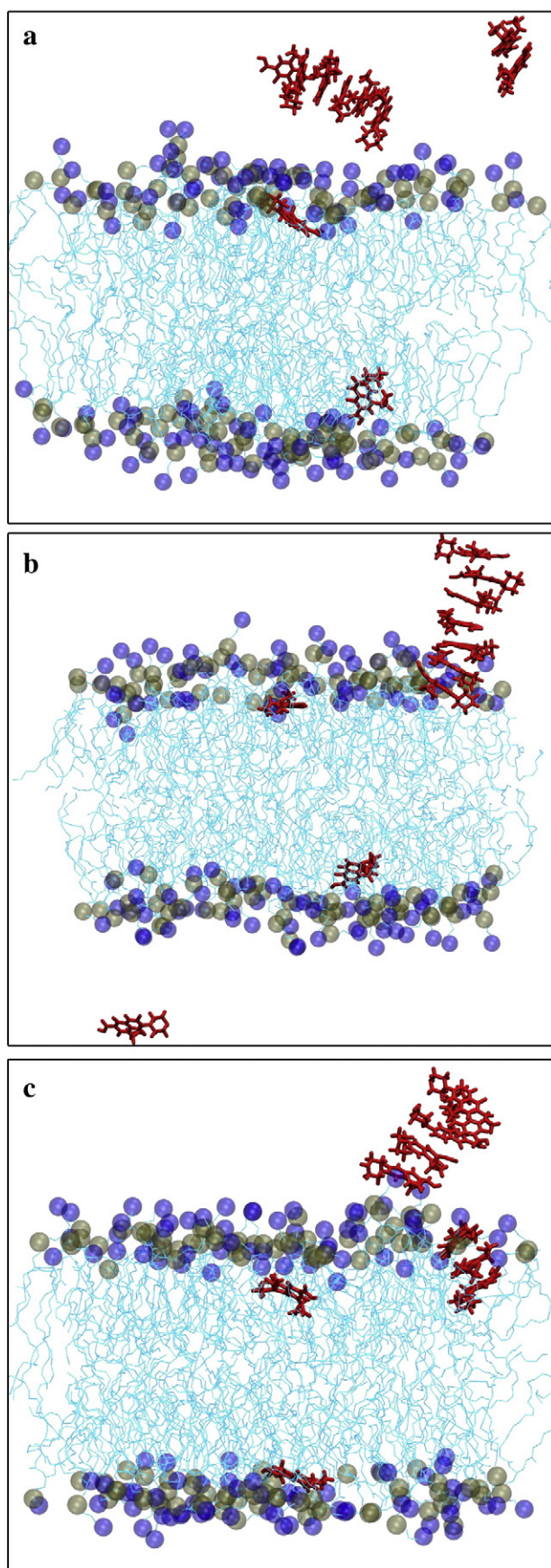

Fig. 2. Distribution along the axis perpendicular to the bilayer (coordinate z) of CPFX molecules (full line) and phosphorus atoms of the lipid headgroups (dotted line). The first 30 ns of the simulation are depicted in plot (a), while plot (b) shows the distribution over the entire simulation (300 ns). Membrane center is at $z = 0$.

(0.08 M), larger and more frequent stacks were observed. Despite experimental observations that have been reported on the stacking of FQs [11,42,43], no atomistic level evidence has been available for this process. However, self-aggregation of drugs was often proven to play a functional role in their activity [43,44] and the same idea can be speculated to hold true also in the case of FQ stacking. Indeed, if we consider a simplified model where zwitterionic CPFX molecules are electric dipoles, it is clear that by their antiparallel association the electric field produced by each dipole would compensate for the field produced by the other. This would result in a reduction of the net electric field measured externally, thus reducing the electrostatic potential of the CPFX complex and favoring their penetration into the less polar environment of the lipid bilayer. A similar effect was presented for the halothane anesthetic in which case partial cancelation of molecular dipole moments through stacking determined the localization of a two molecules stack in the hydrophobic region of the target protein [44]. Additionally, the authors of ref. [44] identified pairing of the halothane molecules by electrostatic interaction to be a potential cause of the annihilation of the anesthetic action of the drug.

3.3. Free energy rofiles

The free energy profiles of monomeric CPFX, zwitterionic and neutral, are shown in Fig. 5. In both cases the excess free energy rises slightly as CPFX enters the head group region amounting to 3.8 kJ/mol (about 1.5 k_BT) for the neutral case and almost twice this value (6.5 kJ/mol, corresponding to 2.6 k_BT) for the zwitterionic one. As CPFX moves deeper into the bilayer, the free energy decreases and the global minimum is reached within the leaflet in the high-density region of the acyl chains. Double bonds of unsaturated lipids are typically localized in this region. The zwitterionic form exhibits a minimum, which is slightly closer to the head group region than in the neutral case. However, the drop in free energy is modest for zwitterionic CPFX, resulting in a positive excess free energy when located in the center of the bilayer, suggesting a strong incompatibility with this region. Instead, free energy calculations confirm that zwitterionic CPFX prefers being in the water phase. On the contrary, the value of −14 kJ/mol (−6 k_BT) obtained for neutral CPFX clearly indicates, in agreement with equilibrium MD simulations, that neutral CPFX can penetrate into the lipid bilayer and that the process is energetically favorable.

Deeper in the bilayer, close to its center, the free energy for the neutral drug form rises, still remaining below 8 kJ/mol (3.2 k_BT). As the free energy barrier is comparable to thermal energy, neutral CPFX is able to translocate through the membrane in reasonable time scales. Full translocation events were not observed in the present MD simulations, but as Fig. 2b highlights, the neutral form of CPFX spends quite extensive periods of time in the vicinity of the membrane center, suggesting that translocations would be observed over time scales of the order of microseconds or larger.

The barrier for zwitterionic CPFX is almost one order of magnitude higher (72.7 kJ/mol, about 29 k_BT) compared to the neutral case, and translocation of these molecules is expected to be at most a rare event. The height of the barrier for zwitterionic CPFX was further confirmed with a short umbrella sampling simulation, which yielded similar results.

Fig. 3. Snapshots of MD simulation showing a stack of neutral CPFX (a) approaching and (b) entering the lipid bilayer. (c) Subsequent rupture of CPFX stacks during the early stages of bilayer penetration, showing that only individual CPFX molecules eventually translocate through the membrane. CPFX molecules are shown in red. Light blue chains represent the hydrophobic region of the bilayer and nitrogen (pink) and phosphorous (green) atoms represent the hydrophilic region. Water molecules as well as PC hydrogens have been omitted for clarity.
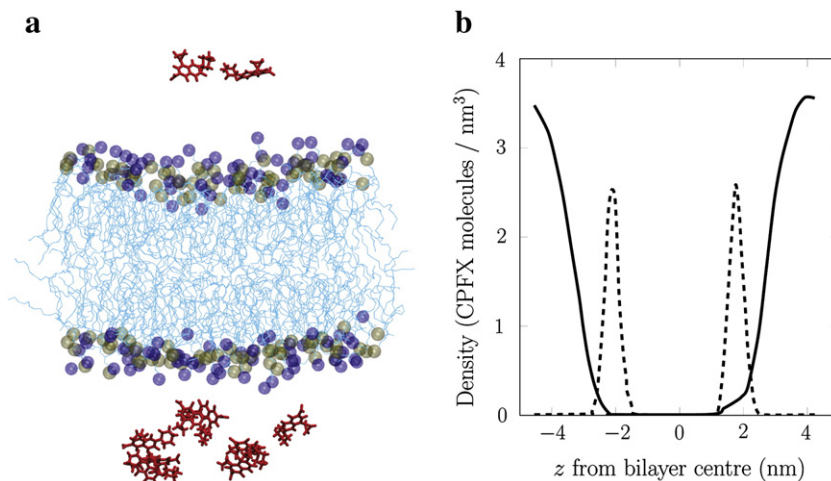
a

b

Fig. 4. (a) Selected snapshot taken at the end of a 300 ns MD simulation revealing zwitterionic CPFX in the water phase aggregated in stacks. (b) Density distribution of zwitterionic CPFX (full line) and phosphorous atoms in lipids (dotted line). Membrane center is at $z = 0$.

3.4. CPFX inside the bilayer

The free energy simulations allow us to investigate several characteristics of CPFX at different depths in the membrane. Fig. 6 reveals that the molecules rotate freely in the water phase, while inside the bilayer there are some clear tendencies. The zwitterionic molecule tends to align perpendicular to the membrane normal to compensate for its charges. This holds inside the bilayer down to about 0.4 nm from the membrane center, where zwitterionic CPFX suddenly changes its orientation, aligning itself to be in parallel to the membrane normal. We discuss this behavior below in more detail. Meanwhile, the neutral drug aligns mostly parallel to the membrane normal, maximizing its hydrophobic interactions with the acyl chains.

The lateral diffusion coefficient of the drug inside the membrane can be calculated from the free energy simulations despite the constraint with respect to the z axis. Both degrees of freedom along the x and y axes in the membrane plane are retained, and thus the lateral diffusion coefficient can be calculated from the mean squared displacement (MSD) of the atoms in the xy plane as a function of time. In each case, a trajectory over 7.5 ns, representing the second half of each simulation was used in the calculation and the fit was performed to the MSD data starting from 50 ps to 1 ns. The obtained results

indicate that both forms of CPFX exhibit quite fast lateral diffusion inside the membrane. We find diffusion coefficients to be in the order of 10^{-6} cm^2/s (see Fig. 7), which is one order of magnitude larger than the lateral diffusion of lipids in fluid-phase (cholesterol-poor) membranes. Also, our results indicate that in the core region of the bilayer, neutral CPFX moves faster than zwitterionic one, promoting its chances for permeation through the free energy barrier in the center of the membrane. As longer free energy simulations would be appropriate for a quantitative estimation of lateral diffusion coefficients, we have validated our results by comparing the lateral diffusion coefficients of lipids with the ones obtained from free energy calculations. A simulation over 140 ns was found to yield a lipid lateral diffusion coefficient of 1.05×10^{-7} cm^2/s, which, considering the large size of a lipid molecule, compares reasonably well with the value of 1.54×10^{-7} cm^2/s obtained from free energy calculations. The lipid diffusion coefficient we found is also in very good agreement with experimental values that range around 1×10^{-7} cm^2/s [45,46] for numerous phospholipids close to physiological temperature. When free energy estimates for lateral diffusion are considered for molecules that are smaller than lipids, one expects smaller deviations, highlighting that the main qualitative conclusions outlined above for CPFX are therefore valid.
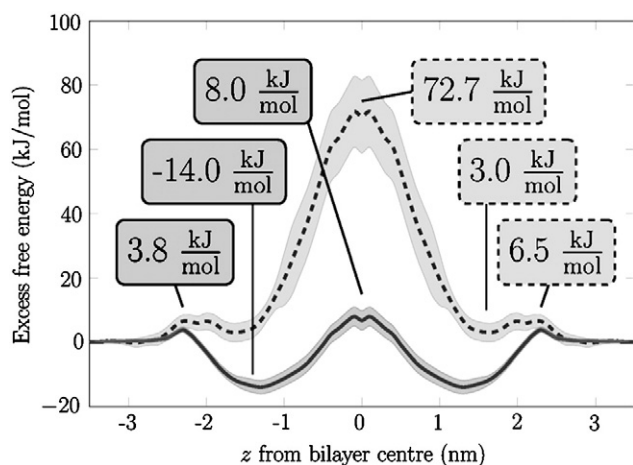

Fig. 5. Excess free energy of both zwitterionic (dashed line) and neutral (full line) CPFX molecules as a function of distance from the center of the bilayer. The curves are mirrored to show the values in the whole bilayer system. Error limits are drawn as gray areas. Key values of the curves are explicitly listed in the figure. Membrane center is at $z = 0$.
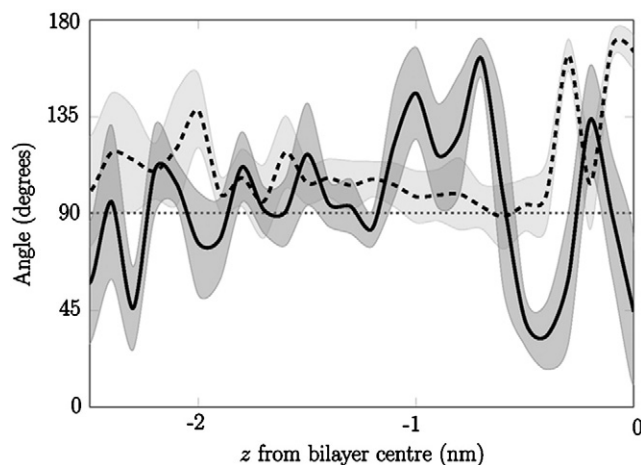

Fig. 6. Angle between the vector from the carbon of the carboxylic group to the nitrogen of the secondary amine group and the z axis at different constraint depths. Data for the zwitterionic and neutral forms of CPFX are drawn in dashed and continuous lines, respectively. Standard deviation is shown as gray areas around the curves. Membrane center is at $z = 0$.
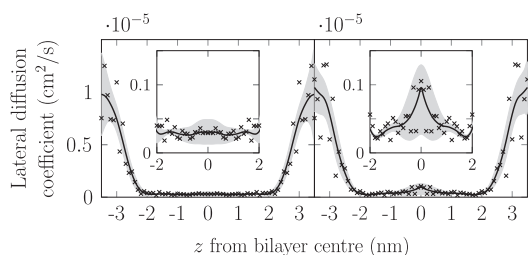
Fig. 7. Lateral diffusion coefficients of zwitterionic (left) and neutral (right) CPFX inside the membrane (its center being at z = 0), the data for lateral diffusion being shown here for varying distances from the membrane center. The solid line is to guide the eye, representing the running average of lateral diffusion coefficient values marked with "x". In the same manner, the shaded area represents the running average of the error limits. These limits are obtained for individual z values as a difference of the two diffusion coefficient values obtained from fits to the two halves of the total fitting interval.

Analysis of hydrogen bonding offers a possible reason for this behavior. It can be seen from Fig. 8 that neutral CPFX loses hydrogen-bonded water molecules as it permeates into the bilayer. Essentially, the number of hydrogen bonds becomes zero in the center of the membrane. This is however not the case for the zwitterionic form of the molecule (see Fig. 8) which retains several water molecules (~7 hydrogen bonds with water) even in the very hydrophobic center of the membrane. Consequently, zwitterionic CPFX appears to remain connected to the water phase from both interfaces of the bilayer, which obviously hinders its diffusive motion.

Hydrogen bonding between CPFX and lipid molecules appears to be small and there is no substantial difference between the neutral and zwitterionic forms. Nevertheless, one can see from Fig. 8 that hydrogen bonding of neutral CPFX with the lipids increases in the headgroup region and can contribute, as discussed in Section 3.1, to the penetration of the molecules into the membrane.

A closer look at the hydrogen bonding pattern of zwitterionic CPFX offers additional insight into the high translocation barrier (Fig. 5) experienced by this form of the molecule. In Fig. 9 we present snapshots of both zwitterionic and neutral CPFX molecules together with water molecules. The pictures describe situations where the drug molecules are either in the center of the bilayer or 0.4 nm from the center. As can be seen, the behavior is very different between the two cases. Closer to the interface (z = 0.4 nm) both CPFX forms are bound to water molecules but exhibit a different orientation which, in the case of the zwitterionic form (oriented perpendicular to membrane normal, Fig. 9c), facilitates formation of hydrogen
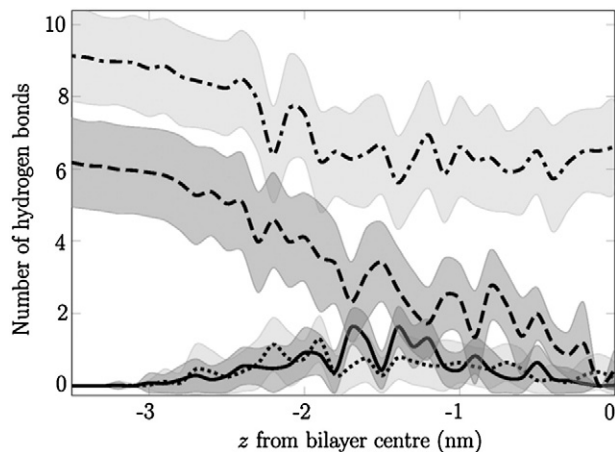
bonds with both polar ends of the molecules. At the same time, neutral CPFX stands upright along the membrane normal (Fig. 9a).

When the drug molecules are pulled to the center of the bilayer (z = 0), their behavior is drastically different. While neutral CPFX is completely depleted of water molecules (Fig. 9b), zwitterionic CPFX reorients from being parallel to the membrane plane to a position where it is parallel to the membrane normal (Fig. 9d), and by doing so it forms water-strings to both water–membrane interfaces of the bilayer. As the sudden reorientation takes place (z changing from 0.4 to 0.0 nm), about half of the hydrogen bonds with water are broken and then reformed on the other side of the bilayer (Fig. 9d). Considering that in the center of the membrane zwitterionic CPFX has ~7 hydrogen bonds with water, with about half of them at each end, one can make a crude estimate of the translocation barrier as 3.5 times the energy of a hydrogen bond. With the formation of a single hydrogen bond being accompanied by the release of 12–24 kJ/mol of enthalpy [47], we obtain an energy barrier of about 42–84 kJ/mol that is in the same ballpark as the computed one (72.7 kJ/mol). This comparison is not conclusive since the enthalpic value does not include a contribution due to changes in entropy, but it yet highlights that the major translocation barrier of zwitterionic CPFX is largely due to the formation of water defects connecting CPFX to bulk water on both sides of the lipid membrane. Related findings have been found for lipid flip-flops and translocation of charged and polar amino acids [48,49].

3.5. Quantum mechanical studies for CPFX monomers and complexes

In order to get a better understanding of the importance of stack formation on the interaction of CPFX with lipid membranes, we employed DFT to calculate the electrostatic potential of CPFX in a dielectric continuum. Calculations were performed on both neutral and zwitterionic monomers as well as on stacks of two or three zwitterionic CPFX molecules. The mapping of the potential on the van der Waals surface is shown in Fig. 10.

Considering first CPFX monomers, we found a high accumulation of charge on the zwitterionic CPFX in water as compared to the neutral form. The extreme values of the potential are almost tripled for the zwitterionic case compared to the neutral one, and they are localized mainly on the carboxyl and piperazine substituents (the two polar ends of the CPFX molecule). Thus, our observation that zwitterionic CPFX does not readily approach the bilayer is not surprising given its large localized charges, which make it appear basically as a dipole. However, stacking of zwitterionic CPFX molecules in the observed anti-parallel arrangement changes the picture considerably. Stacking lowers the electrostatic potential significantly (Fig. 10) in the case of the dimer. Despite still high extreme values on piperazine, the overall potential of the group appears significantly reduced. In Fig. 10 this is visualized as large green areas which correspond to values of ~1 V. Also the electrostatic potential on the carboxyl substituents is reduced, with the highest values lowered by 30%. The reduction of the electrostatic potential is even more pronounced for the sandwiched molecule in the trimer stack, where the potential is decreased by almost one order of magnitude as compared to an isolated individual zwitterionic CPFX. At the same time the extreme values in the trimer are also lowered by almost 30% on both polar ends of the molecules. Not surprisingly, also stacking in vacuum turned out to have basically the same effect on the electrostatic potential despite some differences in the absolute values.

The above QM analysis brings about the reduction of the electrostatic potential during stack formation, thus highlighting that the role of stacking is likely very important in translocation of FQs through lipid bilayers. However, once zwitterionic stacks approach the bilayer and start to enter it, they begin to lose the beneficial effect of solvation, which is known to contribute greatly to the stability of zwitterions. Given this, are zwitterionic stacks stable in the membrane environment?
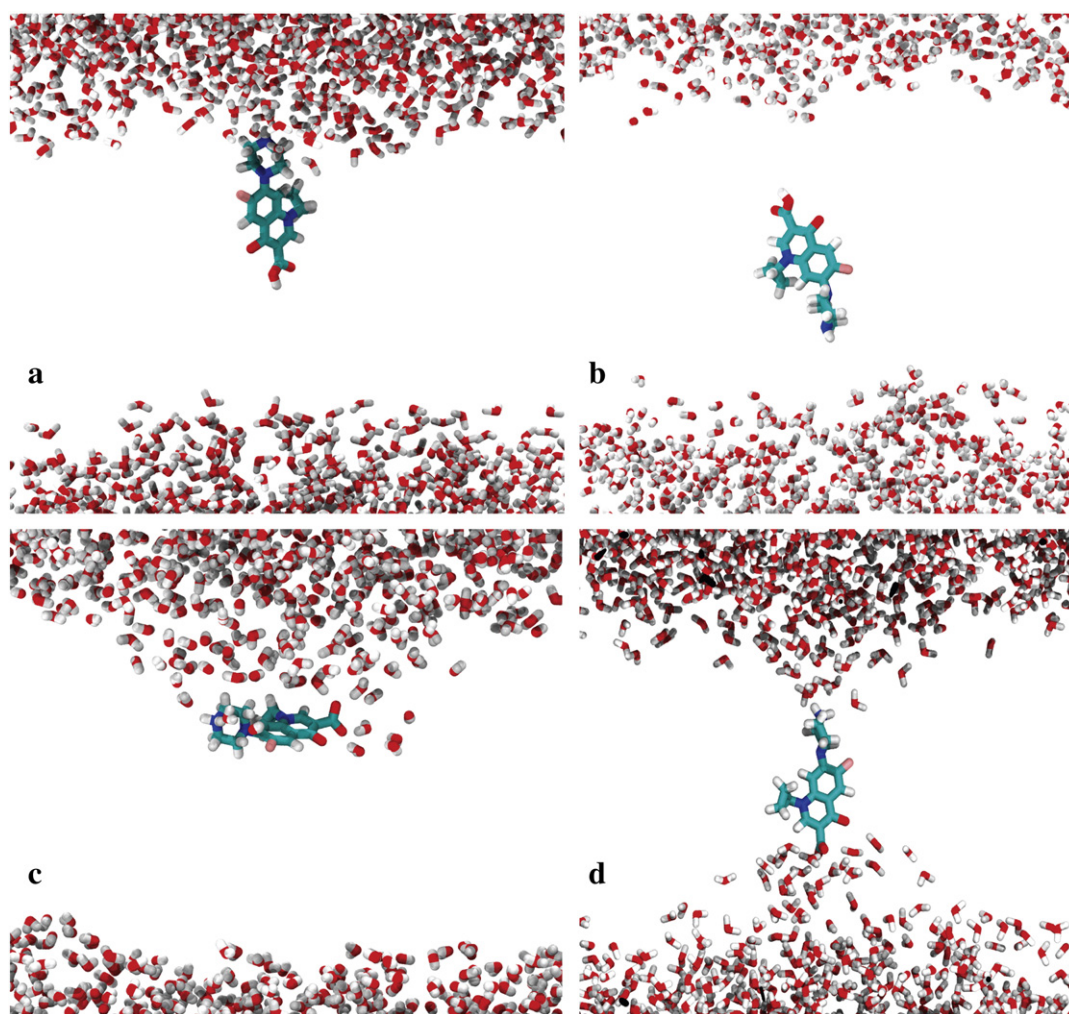

Fig. 8. Number of hydrogen bonds of CPFX in water and lipid phases: neutral CPFX with membrane (solid line); zwitterionic CPFX with membrane (dotted line); neutral CPFX with water (dashed line); zwitterionic CPFX with water (dash–dot line).

Fig. 9. Snapshots of neutral (a, b) and zwitterionic (c, d) CPFX and water molecules taken in the center of the membrane (b, d) and at a distance of 0.4 nm from the center (a, c). For clarity, lipids are not shown.

To address this question, we carried out further QM calculations on zwitterionic dimers in the gas phase and also in implicit solvents with different permittivity. We found that zwitterionic dimers appeared to be not very stable in the gas phase. A simple geometry optimization of two stacked CPFX molecules in vacuum yielded two neutral dipolar molecules, due to intermolecular transfer of protons. In a dielectric continuum, proton transfer was observed upon geometry optimization with dielectric constants up to ~15, but not beyond ~20. That is, stacks of zwitterionic CPFX are stable only in polar environments, with dielectric constants of $\varepsilon \sim 20$ and larger. This implies that stacks are not stable in the membrane interior nor in the lipid head group region having dielectric constants of $\varepsilon \sim 2$–4 and $\varepsilon \sim 12$–18, respectively [50,51]. Instead, they are expected to be stable in the water phase.

To consider this further, we performed DFT calculations in the presence of a few explicit water molecules. Intermolecular proton transfer was prevented if a large enough number of water molecules were added to the system. CPFX dimer stacks surrounded by a shell of 1.7 Å of water molecules (approximately 4–5 molecules located around carboxylic groups) still underwent intermolecular proton transfer. When we included water within a distance of 2 Å (about 15 molecules out of which 4 around piperazine and one around carboxyl), stabilization of the zwitterions was achieved. The number of water molecules coincides with the one shown by the DFT studies of Lambert et al. to stabilize levofloxacin [52]. According to our analysis of CPFX–water hydrogen bonding, even a single zwitterionic

CPFX would not be stabilized by water molecules since ~3.5 hydrogen bonds are observed at each of its polar ends. Summarizing, the proton transfer observed in our QM calculations appears to be a highly probable process as CPFX stacks cross the water–membrane interface and penetrate the membrane.

4. Conclusions

Concluding, our data provide compelling evidence that only the neutral form readily permeates through a lipid bilayer. The translocation process starts from the water phase where CPFX molecules appear as stacks. Close to a membrane they form hydrogen bonds with the lipid head groups. The pattern of these hydrogen bonds points to the role of piperazine in initiating the translocation process, which explains the enhanced permeability of piperazin substituted FQs observed in experiments [37–40]. Zwitterionic CPFX molecules partition mainly to the water phase due to their strongly polar nature. However, charge distribution arising from their interaction and subsequent stack formation significantly reduces the polarity of the stacks potentially favoring their insertion into the bilayer. This would presumably reduce the difference in the energetic barrier upon entering the bilayer, which was revealed by free energy calculations to be almost twice as large for a single zwitterionic CPFX molecule as compared to a neutral one.

To move on, ciprofloxacin molecules diffuse through a lipid membrane in their neutral form, neutralization taking place due to
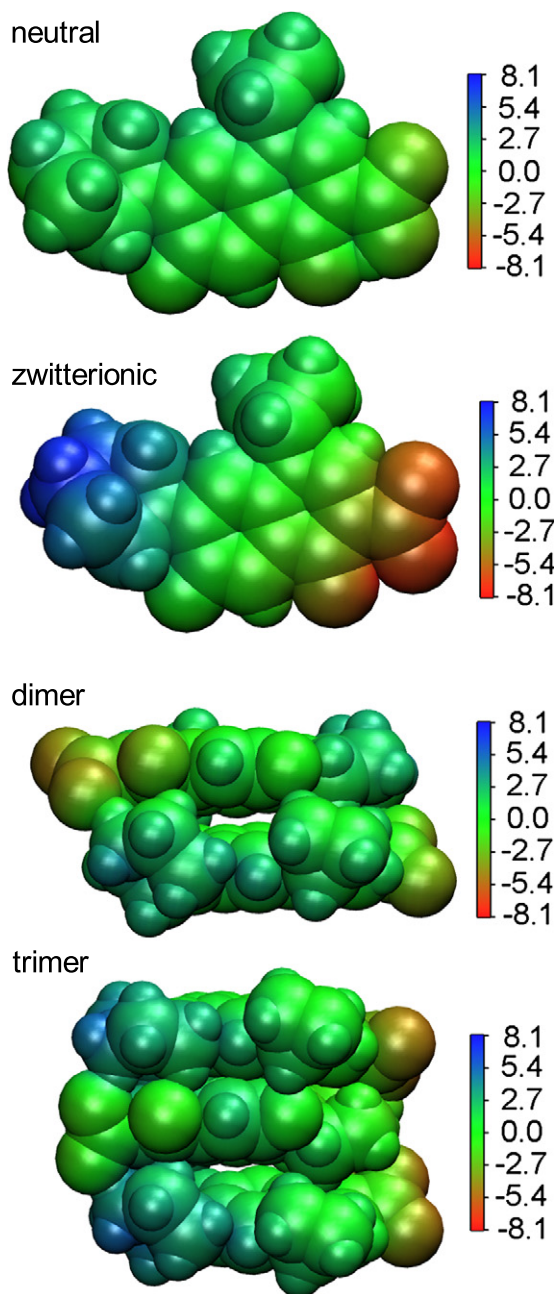
Fig. 10. Electrostatic potential maps at the molecular van der Waals surface in a dielectric continuum corresponding to the water phase (dielectric constant 80). Starting structures for DFT optimization were taken from classical all-atom simulations. Electrostatic potential values are given in units of Volt.

[53], the proposed mechanism can be considered as the dominant one as it explains also experiments that involve model lipid bilayers and FQs alone.

We have provided here an in-depth picture for the interaction of lipid bilayers with a major FQ, ciprofloxacin. We have elucidated one of the fundamental issues regarding the diffusion mechanism of such drugs through cellular membranes. Important to stress here is that the present results go beyond the class of FQs alone, as the suggested mechanism can largely contribute to the diffusion of many other ampholitic drugs with stacking tendencies. With ampholytes being a rule rather than an exception in biochemistry, and with the large diversity of ampholytic drugs on the market, the importance of understanding the interaction of such compounds with cellular membranes cannot be overestimated. The rationalization of the mechanism of interaction and translocation of ampholytes outlined here is expected to contribute to biochemistry and medicinal chemistry in particular, when more potent drugs are being developed.

Acknowledgements

References

[1] H. Nikaido, D.G. Thanassi, Penetration of lipophilic agents with multiple protonation sites into bacterial cells: tetracyclines and fluoroquinolones as examples, Antimicrob. Agents Chemother. 37 (1993) 1393–1399.
[2] M. Dechène, H. Leying, W. Cullmann, Role of the outer membrane for quinolone resistance in enterobacteria, Chemotherapy 36 (1990) 13–23.
[3] P. Neves, E. Berkane, P. Gameiro, M. Winterhalter, B. de Castro, Interaction between quinolones antibiotics and bacterial outer membrane porin OmpF, Biophys. Chem. 113 (2005) 123–128.
[4] J.L. Vázquez, S. Merino, O. Domenech, M. Berlanga, M. Viñas, M.T. Montero, J. Hernández-Borrell, Determination of the partition coefficients of a homologous series of ciprofloxacin: influence of the n − 4 piperazinyl alkylation on the antimicrobial activity, Int. J. Pharm. 220 (2001) 53–62.
[5] K.Y. Tam, A. Avdeef, O. Tsinman, N. Sun, The permeation of amphoteric drugs through artificial membranes—an in combo absorption model based on paracellular and transmembrane permeability, J. Med. Chem. 53 (2010) 392–401.
[6] A. Pagliara, P.-A. Carrupt, G. Caron, P. Gaillard, B. Testa, Lipophilicity profiles of ampholytes, Chem. Rev. 97 (1997) 3385–3400.
[7] J. Sun, S. Sakai, Y. Tauchi, Y. Deguchi, J. Chen, R. Zhang, K. Morimoto, Determination of lipophilicity of two quinolone antibacterials, ciprofloxacin and grepafloxacin, in the protonation equilibrium, Eur. J. Pharm. Biopharm. 54 (2002) 51–58.
[8] J. Sun, S. Sakai, Y. Tauchi, Y. Deguchi, G. Cheng, J. Chen, K. Morimoto, Protonation equilibrium and lipophilicity of olamufloxacin (HSR-903), a newly synthesized fluoroquinolone antibacterial, Eur. J. Pharm. Biopharm. 56 (2003) 223–229.
[9] K. Takács-Novák, B. Noszál, I. Hermecz, G. Keresztúri, B. Podányi, G. Szász, Protonation equilibria of quinolone antibacterials, J. Pharm. Sci. 79 (1990) 1023–1028.
[10] Y.X. Furet, J. Deshusses, J.C. Pechère, Transport of pefloxacin across the bacterial cytoplasmic membrane in quinolone-susceptible staphylococcus aureus, Antimicrob. Agents Chemother. 36 (1992) 2506–2511.
[11] N. Maurer, K.F. Wong, M.J. Hope, P.R. Cullis, Anomalous solubility behavior of the antibiotic ciprofloxacin encapsulated in liposomes: a 1H-NMR study, Biochim. Biophys. Acta 1374 (1998) 9–20.
[12] D.D. Lasic, B. Ceh, M.C. Stuart, L. Guo, P.M. Frederik, Y. Barenholz, Transmembrane gradient driven phase transitions within vesicles: lessons for drug delivery, Biochim. Biophys. Acta 1239 (1995) 145–156.
[13] G. Bouchard, A. Pagliara, P.-A. Carrupt, B. Testa, V. Gobry, H.H. Girault, Theoretical and experimental exploration of the lipophilicity of zwitterionic drugs in the 1,2-dichloroethane/water system, Pharm. Res. 19 (2002) 1150–1159.
[14] T. Róg, H. Martinez-Seara, N. Munck, M. Oresic, M. Karttunen, I. Vattulainen, Role of cardiolipins in the inner mitochondrial membrane: insight gained through atom-scale simulations, J. Phys. Chem. B 113 (2009) 3413–3422.
[15] W.L. Jørgensen, D.S. Maxwell, J. Tirado-Rives, Development and testing of the OPLS all-atom force field on conformational energetics and properties of organic liquids, J. Am. Chem. Soc. 118 (1996) 11225–11236.
[16] G. Kaminski, R.A. Friesner, J. Tirado-Rives, W.L. Jørgensen, Evaluation and reparametrization of the OPLS-AA force field for proteins via comparison with accurate quantum chemical calculations on peptides, J. Phys. Chem. B 105 (2001) 6474–6487.
[17] M.L.P. Price, D. Ostrovsky, W.L. Jørgensen, Gas-phase and liquid-state properties of esters, nitriles, and nitro compounds with the OPLS-AA force field, J. Comput. Chem. 15 (2001) 681–695.
[18] R.C. Rizzo, W.L. Jørgensen, OPLS all-atom model for amines: resolution of the amine hydration problem, J. Am. Chem. Soc. 121 (1999) 4827–4836.

intermolecular transfer of protons favored by total or partial desolvation of neutral and zwitterionic forms, respectively. In the absence of this process, the translocation barrier of zwitterionic CPFX is very high, rendering the translocation of zwitterionic CPFX a rare event. For the neutral molecule, however, translocation can be expected to be quite frequent given that the free energy barrier for translocation is 3.2 k_BT and therefore comparable to thermal energy. The large free energy barrier experienced by zwitterionic CPFX close to the center of the membrane can largely be explained by the formation of water defects on both sides of the membrane and the accompanied breaking of hydrogen bonds as CPFX undergoes motion through the membrane core region. While other factors like chelation with divalent ions or trans-membrane pH gradient have been shown to contribute to the passive diffusion of FQs through the membrane too

[19] Y. Takaoka, M. Pasenkiewicz-Gierula, H. Miyagawa, K. Kitamura, Y. Tamura, A. Kusumi, Molecular dynamics generation of nonarbitrary membrane models reveals lipid orientational correlations, Biophys. J. 79 (2000) 3118–3138.

[20] T. Róg, I. Vattulainen, A. Bunker, M. Karttunen, Glycolipid membranes through atomistic simulations: effect of glucose and galactose head groups on lipid bilayer properties, J. Phys. Chem. B 111 (2007) 10146–10154.

[21] C.I. Bayly, P. Cieplak, W. Cornell, P.A. Kollman, A well-behaved electrostatic potential based method using charge restraints for deriving atomic charges: the RESP model, J. Phys. Chem. 97 (1993) 10269–10280.

[22] P. Cieplak, F.-Y. Dupradeau, Including polarization effects in the RESP charge derivation method, 236th ACS National Meeting, Philadelphia, August 17–August 21, 2008.

[23] M.J. Frisch, G.W. Trucks, H.B. Schlegel, G.E. Scuseria, M.A. Robb, J.R. Cheeseman, G. Scalmani, V. Barone, B. Mennucci, G.A. Petersson, H. Nakatsuji, M. Caricato, X. Li, H.P. Hratchian, A.F. Izmaylov, J. Bloino, G. Zheng, J.L. Sonnenberg, M. Hada, M. Ehara, K. Toyota, R. Fukuda, J. Hasegawa, M. Ishida, T. Nakajima, Y. Honda, O. Kitao, H. Nakai, T. Vreven, J.A. Montgomery Jr., J.E. Peralta, F. Ogliaro, M. Bearpark, J.J. Heyd, E. Brothers, K.N. Kudin, V.N. Staroverov, R. Kobayashi, J. Normand, K. Raghavachari, A. Rendell, J.C. Burant, S.S. Iyengar, J. Tomasi, M. Cossi, N. Rega, N.J. Millam, M. Klene, J.E. Knox, J.B. Cross, V. Bakken, C. Adamo, J. Jaramillo, R. Gomperts, R.E. Stratmann, O. Yazyev, A.J. Austin, R. Cammi, C. Pomelli, J.W. Ochterski, R.L. Martin, K. Morokuma, V.G. Zakrzewski, G.A. Voth, P. Salvador, J.J. Dannenberg, S. Dapprich, A.D. Daniels, O. Farkas, J.B. Foresman, J.V. Ortiz, J. Cioslowski, D.J. Fox, Gaussian 09, Revision B.1, Gaussian, Inc., Wallingford CT, 2009.

[24] W.L. Jørgensen, J. Chandrasekhar, J.D. Madura, R.W. Impey, M. Klein, Comparison of simple potential functions for simulating liquid water, J. Chem. Phys. 79 (1983) 926–935.

[25] E. Lindahl, B. Hess, D.V.D. Spoel, Gromacs 3.0: a package for molecular simulation and trajectory analysis, J. Mol. Model. 7 (2001) 306–317.

[26] D.V.D. Spoel, E. Lindahl, B. Hess, G. Groenhof, A.E. Mark, H.J.C. Berendsen, GROMACS: fast, flexible, and free, J. Comput. Chem. 26 (2005) 1701–1718.

[27] B. Hess, H. Bekker, H.J.C. Berendsen, J.G.E.M. Fraaije, Lincs: a linear constraint solver for molecular simulations, J. Comput. Chem. 18 (1997) 1463–1472.

[28] H.J.C. Berendsen, J.P.M. Postma, W.F. van Gunsteren, A. Dinola, J.R. Haak, Molecular dynamics with coupling to an external bath, J. Chem. Phys. 81 (1984) 3684–3690.

[29] U. Essmann, L. Perera, M.L. Berkowitz, T. Darden, H. Lee, L.G. Pedersen, A smooth particle mesh Ewald method, J. Chem. Phys. 103 (1995) 8577–8592.

[30] K. Murzyn, W. Zhao, M. Karttunen, M. Kurdziel, T. Róg, Dynamics of water at membrane surfaces: effect of headgroup structure, Biointerphases 1 (2006) 98–105.

[31] W. Zhao, T. Róg, A.A. Gurtovenko, I. Vattulainen, M. Karttunen, Atomic-scale structure and electrostatics of anionic palmitoyloleoylphosphatidylglycerol lipid bilayers with Na$^+$ counterions, Biophys. J. 92 (2007) 1114–1124.

[32] TURBOMOLE V6.1 2009, a development of University of Karlsruhe and Forschungszentrum Karlsruhe GmbH, 1989–2007, TURBOMOLE GmbH, since 2007.

[33] S. Grimme, Accurate description of van der Waals complexes by density functional theory including empirical corrections, J. Comput. Chem. 25 (2004) 1463–1473.

[34] S. Grimme, Semiempirical GGA-type density functional constructed with a long-range dispersion correction, J. Comput. Chem. 27 (2006) 1787–1799.

[35] A. Klamt, G. Schüürmann, Cosmo: a new approach to dielectric screening in solvents with explicit expressions for the screening energy and its gradient, J. Chem. Soc. Perkin Trans. 2 (5) (1993) 799–805.

[36] A. Schäfer, A. Klamt, D. Sattel, J.C.W. Lohrenz, F. Eckert, COSMO implementation in Turbomole: extension of an efficient quantum chemical code towards liquid systems, Phys. Chem. Chem. Phys. 2 (2000) 2187–2193.

[37] P. Ball, Quinolone generations: natural history or natural selection? J. Antimicrob. Chemother. 46 (Suppl. T1) (2000) 17–24.

[38] D.T. Chu, P.B. Fernandes, Structure–activity relationships of the fluoroquinolones, Antimicrob. Agents Chemother. 33 (1989) 131–135.

[39] T.D. Gootz, P.R. McGuirk, M.S. Moynihan, S.L. Haskell, Placement of alkyl substituents on the C-7 piperazine ring of fluoroquinolones: dramatic differential effects on mammalian topoisomerase II and DNA gyrase, Antimicrob. Agents Chemother. 38 (1994) 130–133.

[40] M.N. Patel, M.R. Chhasatia, D.S. Gandhi, DNA-interaction and in vitro antimicrobial studies of some mixed-ligand complexes of Cobalt(II) with fluoroquinolone antibacterial agent ciprofloxacin and some neutral bidentate ligands, Bioorg. Med. Chem. Lett. 19 (2009) 2870–2873.

[41] M.D. Prasanna, T.N.G. Row, Hydrogen bonded networks in hydrophilic channels: crystal structure of hydrated ciprofloxacin lactate and comparison with structurally similar compounds, J. Mol. Struct. 559 (2001) 255–261.

[42] A.V. Polishchuk, E.T. Karaseva, T.B. Emelina, V.E. Karasev, The formation of nalidixic acid dimers and excimers in aqueous solutions, Russ. J. Phys. Chem. A 83 (2009) 1064–1068.

[43] W. Caetano, M. Ferreira, M. Tabak, M.I.M. Sanchez, O.N. Oliveira, P. Krüger, M. Schalke, M. Lösche, Cooperativity of phospholipid reorganization upon interaction of dipyridamole with surface monolayers on water, Biophys. Chem. 91 (2001) 21–35.

[44] P. Tang, Y. Xu, Large-scale molecular dynamics simulations of general anesthetic effects on the ion channel in the fully hydrated membrane: the implication of molecular mechanisms of general anesthesia, Proc. Natl. Acad. Sci. U. S. A. 99 (2002) 16035–16040.

[45] G. Lindblom, G. Orädd, A. Filippov, Lipid lateral diffusion in bilayers with phosphatidylcholine, sphingomyelin and cholesterol. An NMR study of dynamics and lateral phase separation, Chem. Phys. Lipids 141 (2006) 179–184.

[46] A. Filippov, G. Orädd, G. Lindblom, Domain formation in model membranes studied by pulsed-field gradient-NMR: the role of lipid polyunsaturation, Biophys. J. 93 (2007) 3182–3190.

[47] G.D. Rose, R. Wolfenden, Hydrogen bonding, hydrophobicity, packing and protein folding, Annu. Rev. Biophys. Biomol. Struct. 22 (1993) 381–415.

[48] J.L. MacCallum, W.F.D. Bennett, D.P. Tieleman, Distribution of amino acids in a lipid bilayer from computer simulations, Biophys. J. 94 (2008) 3393–3404.

[49] A. Gurtovenko, J. Anwar, I. Vattulainen, Defect-mediated trafficking across cell membranes, Chem. Rev. 110 (2010) 6077–6103.

[50] R.B.M. Koehorst, R.B. Spruijt, F.J. Vergeldt, M.A. Hemminga, Lipid bilayer topology of the transmembrane alpha-helix of M13 major coat protein and bilayer polarity profile by site-directed fluorescence spectroscopy, Biophys. J. 87 (2004) 1445–1455.

[51] H. Nymeyer, H.-X. Zhou, A method to determine dielectric constants in non-homogeneous systems: application to biological membranes, Biophys. J. 94 (2008) 1185–1193.

[52] A. Lambert, J.-B. R.de Vains, M.F. Ruiz-Lopez, Structure of levofloxacin in hydrophilic and hydrophobic media: relationship to its antibacterial properties, Chem. Phys. Lett. 442 (2007) 281–284.

[53] M. Fresta, S. Guccione, A.R. Beccari, P.M. Furneri, G. Puglisi, Combining molecular modeling with experimental methodologies: mechanism of membrane permeation and accumulation of ofloxacin, Bioorg. Med. Chem. 10 (2002) 3871–3889.